

Packet-by-packet all-optical burst-mode 3R regeneration in an optical-label switching router

Masaki Funabashi, Zuqing Zhu, Zhong Pan, and S. J. B. Yoo

Department of Electrical and Computer Engineering, University of California, Davis, CA 95616, USA
yoo@ece.ucdavis.edu

Abstract: This paper demonstrates 10 Gb/s packet-by-packet burst-mode optical 3R regeneration in an optical-label switching router, achieving bit-error-rates below 1×10^{-9} with the guard time ranging from 50 to 1000 ns despite clock-phase discontinuity between packets.

©2006 Optical Society of America

OCIS codes: (060.4250) Networks, (060.4510) Optical communications

1. Introduction

Optical packet switching is of strong interest due to its potentials for flexibility, scalability, and bandwidth efficiency. Optical-label switching (OLS) is an attractive technology that takes advantage of flexible label processing in the electrical domain for routing and packet forwarding decisions while achieving high-capacity data payload forwarding in the optical domain. All-optical signal regeneration plays an important role in scalable all optical networking. While optical 2R regeneration (reamplification, reshaping) is often sufficient [1], full 3R regeneration functionality including retiming is critically important for high bit-rate systems where jitter accumulations are detrimental. 3R regenerators in high-capacity asynchronous optical packet switching systems require packet-by-packet burst-mode operation in support of variable-length packets arriving at random time with short guard-time. This paper demonstrates error-free operation of all-optical packet-by-packet burst-mode 3R regeneration over a wide range of guard-time of 50 nsec – 1000 nsec in an optical-label switching router.

2. Experimental Setup and Results

The experimental setup utilized a practical situation where the burst-mode 3R regenerator is part of an optical label switching router [2]. Fig. 1 shows the experimental setup. A subcarrier-multiplexing transmitter (SCM-Tx1) generates optical packets with 10 Gb/s payload on the baseband and 155 Mb/s label on the 14 GHz subcarrier. The fiber Bragg grating (FBG) based label extractor (LE1) separates the optical label from the payload, and the burst-mode label receiver (BMRx1) receives the optical label. The switch-controller makes a decision according to the label content and the forwarding table, and instructs the tunable wavelength converter (TWC1) to tune to a new wavelength corresponding to directing the payload to a desired output port of the arrayed waveguide grating router (AWGR). $(m,n)_{in}$ and $(m,n)_{out}$ represent the n -th wavelength channel on the m -th input and output fiber, respectively. The fixed wavelength converter (FWC) at the AWGR output converts the payload wavelength to a desired fixed wavelength. Here we propose to incorporate the burst-mode 3R functionality in the FWC.

The proposed burst-mode 3R regenerator consists of an all-optical 2R regeneration stage and the burst-mode retiming stage [3]. The first 2R stage is a semiconductor optical amplifier based Mach-Zehnder interferometer (SOA-MZI) operating in a differential mode, which offers faster device response than the gain recovery time of the SOAs. The tunable delay line (TDL2) adjusts a relative delay between the two arms. The retiming stage of the 3R regenerator includes the burst-mode clock recovery module utilizing the Fabry-Perot filter (FPF) and an SOA [4] and the synchronous modulation module using the LiNbO₃ modulator (LN). The FPF has a comb-like periodical transmission function with respect to the optical frequency. By design, its free spectral range (FSR) matches the bit-rate of the incoming payload (i.e. 10 GHz) and its finesse is approximately 100 [5]. According to its periodical transmission characteristics, the FPF extracts the line spectral components at the optical carrier and the overtones at the clock frequencies, and it transmits a clock-like optical signal. The temperature tuning and stabilization of the FPF maintain the spectral alignment of one of the pass-bands with the optical carrier frequency. Due to the polarization dependence of the FPF, the polarization controller (PC1) is used to align the input polarization to one of the two principal axes of the FPF. The transmitted clock signal just after the FPF exhibits amplitude variations following the pattern of the incoming bit stream. A gain-saturated SOA following the FPF greatly suppresses the amplitude variations when sufficiently high (> 3 dBm) input power signal is injected into the SOA. The subsequent band-pass filter (BPF3) transmits the recovered clock signal and effectively suppresses amplified spontaneous emission (ASE) noise from the SOA especially during the guard-time. The O/E receiver converts the optical clock signal into an electrical signal that modulates the LN through the LN driver. Fig. 2(a) shows the rising edge and the

falling edge of the recovered clock measured at the output of the retiming stage where the LN is modulated by the recovered clock. The rise and fall times defined as the transition time between the 10 and 90% levels are approximately 800 ps and 34 ns, respectively. To achieve a short and pattern-independent rise time of the recovered clock, we used a preamble of 16-bit consequent ones ('1's) followed by a pseudo random bit sequence (PRBS) $2^{23}-1$ data until the end of each packet. To synchronize the payload arrival at the LN with the recovered clock, the fiber length and the TDL3 are adjusted. As Fig. 2(b) shows, the entire packet bits reside where the recovered optical clock signal stays stable (>90% level). The fine-tuning of TDL3 allows matching of the phase between the recovered clock and the payload signal so that the synchronous modulation carves out the center portions of the payload return-to-zero (RZ) pulses.

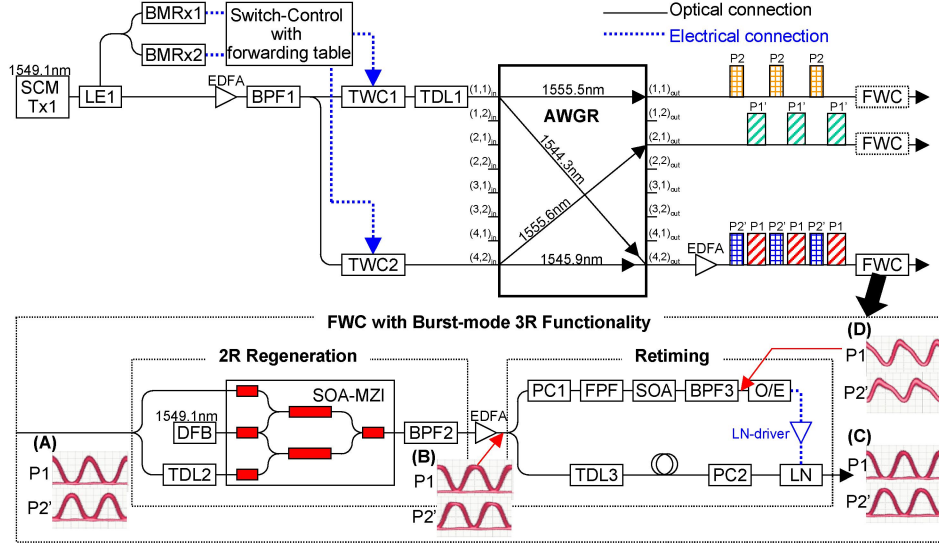


Fig. 1. Experimental setup of the optical-label switching router with the 3R regenerator (SCM-Tx: Subcarrier multiplexing transmitter, LE: Label extractor, EDFA: Erbium-doped fiber amplifier, BMRx: Burst-mode receiver, LN: LiNbO₃ modulator, BPF: Optical band-pass filter, TWC: Tunable wavelength converter, TDL: Tunable delay line, AWGR: Arrayed waveguide grating router, FWC: Fixed wavelength converter, DFB: Distributed feedback laser, SOA-MZI: Semiconductor optical amplifier based Mach-Zehnder interferometer, PC: Polarization controller, FPF: Fabry-Perot filter, O/E: optical-electrical receiver)

We experimentally emulate the situation where two packets with mutually out-of-phase clock cycles arrive at the burst-mode 3R regenerator with guard-time as a parameter. Packets P1 and P2 of differing packet lengths are alternatively generated as the 10 Gb/s RZ payload (P1: 21504 bits; P2: 16128 bits). The guard times between P1 and P2 (and between P2 and P1) are constant for each experiment, but various guard-times of 50, 100, 200, 500, and 1000 ns have been experimented. For simplicity, an identical payload sequence from the SCM-Tx1 feeds both TWC1 and TWC2. The TWC1 switches the P1 to the output port (4,2)_{out} and P2 to (1,1)_{out} while TWC2 switches P1' to (2,1)_{out} and P2' to (4,2)_{out}. By adjusting the TDL1, the relative clock phase difference between P1 and P2' is set at π (50 ps shift). This is the largest possible phase discontinuity and thus thought to be the worst and the most difficult case for the burst-mode clock recovery, because unsuccessful clock recovery with improper clock phase will result in destructive synchronous modulation in the retiming stage. Fig. 3 shows eye diagrams measured (a) before and (b) after the 2R regeneration, (c) after retiming, and (d) recovered optical clock when the guard time is 50 ns. Peak positions of the P2' pulses are shifted by 50 ps, compared to those of the P1 pulses, indicating that the clock recovery can follow the phase jumps. The eye diagrams after the retiming for both P1 and P2' exhibit excellent extinction ratios and clear eye openings. The pulse shape after the 2R regeneration is intentionally broadened in time to realize a relatively flat mark level. This is preferable for the synchronous modulation, where the pulse edges of the broadened pulse are chopped off by the recovered clock. For all cases of the guard time of 50, 100, 200, 500, and 1000 ns, clear eye diagrams are observed at each stage. Bit-error-rate (BER) curves for both P1 and P2' are also measured at two locations: before the 2R stage and after the retiming stage in all the cases of 50-1000 ns guard times (Fig. 4(a) and (b)). Since the BER tester (BERT) cannot synchronize simultaneously with P1 and P2' due to the clock phase difference, the BER curves for P1 and P2' are measured separately using the local clock trigger from the BERT. As Fig. 4(b) shows, all BER curves show error-free performance below 1×10^{-9} , and the relative penalties are within 2 dB range of the calibrated received power when the average received power is recalibrated considering the duty cycle variations due to differing guard-times. The BER curves after retiming shows nearly zero or even slightly

negative penalty compared to those before the 2R regeneration. We also experimentally verified that tuning of the TDL1 over one bit period (100 ps) showed no observable difference in the measured BER values, and that similar experiments with a standard O/E/O 3R regeneration failed to provide successful clock recovery and BER measurements in many of the cases tested above for all-optical 3R regeneration. The root-mean-square (RMS) jitter of the recovered optical clock that is measured preliminary with continuous PRBS $2^{23}-1$ data is 0.342 ps.

3. Conclusion

We have demonstrated, for the first time, an all-optical burst-mode 3R regeneration in the optical label switching router with error-free performance below 1×10^{-9} over a wide guard time range from 50 to 1000 ns regardless of the presence of phase jump between packets.

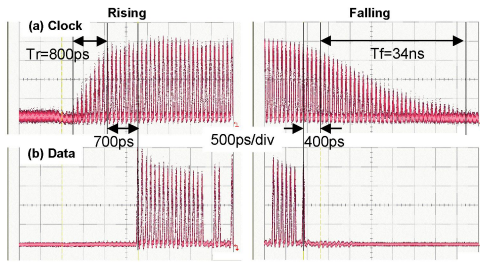


Fig. 2. (a)Rising and falling parts of the recovered clock signal (b)Packet data aligned within the stable part of the recovered clock.

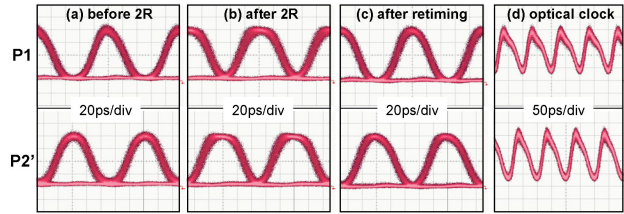


Fig. 3. Eye diagrams measured (a) before (point A in Fig. 1) and (b) after (point B) the 2R regeneration, (c) after retiming (point C), and (d) after the optical clock recovery (point D). PRBS $2^{23}-1$ pattern without the preamble is used for this measurement.

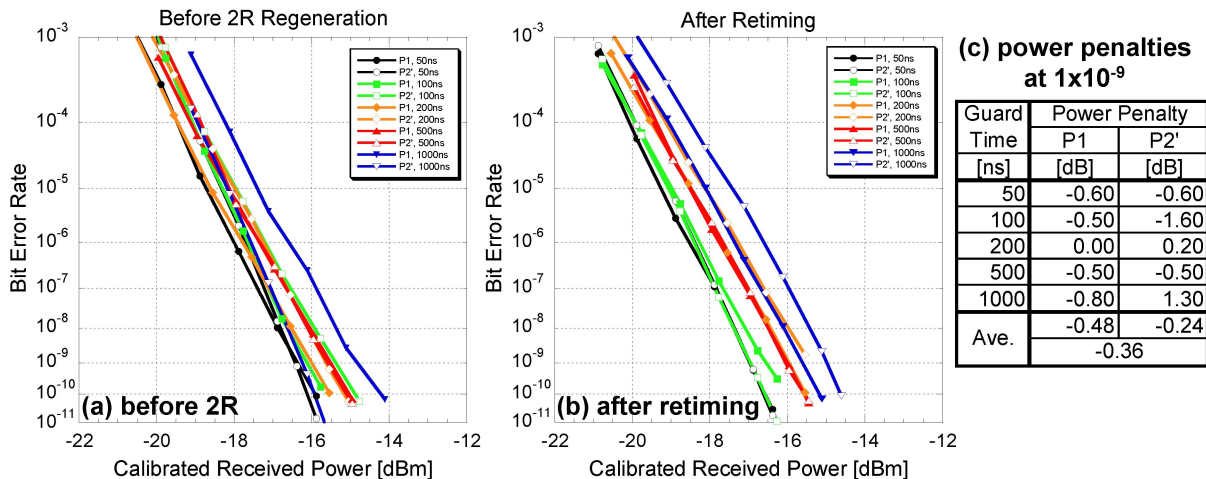


Fig. 4. BER curves measured (a) before the 2R stage (point A in Fig. 1) and (b) after the retiming stage (point C), and (c) power penalties at $BER=1 \times 10^{-9}$.

References

- [1] M. Y. Jeon, *et al.*, "Demonstration of all-optical packet switching routers with optical label swapping and 2R regeneration for scalable optical label switching network applications," *J. Lightwave Technol.*, **21**, 2723-2733 (2003).
- [2] Z. Pan, *et al.*, "Packet-by-packet wavelength, time, space-domain contention resolution in an optical-label switching router with 2R regeneration," *IEEE Photon. Technol. Lett.*, **15**, 1312-1314 (2003)
- [3] M. Funabashi, *et al.*, "All-optical 3R regeneration in monolithic SOA-MZI to achieve 0.4 million km fiber transmission," in *Technical Digest of IEEE LEOS Annual Meeting*, paper MM3 (2005).
- [4] G. Contestabile, *et al.*, "40-GHz all-optical clock extraction using a semiconductor-assisted Fabry-Perot filter," *IEEE Photon. Tech. Lett.*, **16**, 2523-2525 (2004).
- [5] C. Bintjas, *et al.*, "Clock recovery circuit for optical packets," *IEEE Photon. Technol. Lett.*, **14**, 1363-1365 (2000).

Acknowledgment

This work was supported in part by NSF NRT 0335301 and OIDA PTAP, which is supported by NSF and DARPA MTO.